Mon. Not. R. Astron. Soc. **303,** 301–308 (1999)

Limits on dust and metallicity evolution of Lyα forest clouds from *COBE*

Andrea Ferrara,[1⋆] Biman Nath,[2⋆] Shiv K. Sethi[3⋆] and Yuri Shchekinov[1,4⋆]

[1] *Osservatorio Astrofisico di Arcetri, Largo E. Fermi 5, 50125 Firenze, Italy*
[2] *Raman Research Institute, Bangalore – 560080, India*
[3] *Institut d'Astrophysique, 75014 Paris, France*
[4] *Department of Physics, Rostov State University, 344090 Rostov on Don, Russia*

Accepted 1998 October 15. Received 1998 October 15; in original form 1998 April 6

ABSTRACT

We consider the possible observational consequences of dust and metals in Lyα forest clouds. We relate the dust content, $\Omega_{\rm d}^{\rm Ly\alpha}$, to the metal evolution of the absorbers and assume that dust is heated by the ultraviolet background radiation and by the cosmic microwave background (CMB). We find that the dust temperature deviates from $T_{\rm CMB}$ by at most 10 per cent at redshift $z = 0$. The Lyα cloud dust opacity to redshift $\sim$5 sources around the observed wavelength $\lambda_0 \sim 1\mu$m is $\tau \sim 0.13$, and could affect observations of the distant universe in that band. The expected CMB spectral distortions arising from high-z dust in Lyα clouds is $\sim$1.25–10 smaller than the current *COBE* upper limit, depending on the metallicity evolution of the clouds. If Lyα clouds are clustered, the corresponding CMB anisotropy due to dust is $\sim 10^{-1}$ on angular scales $\theta \lesssim 10$ arcsec at frequencies probed by various future/ongoing far-infrared (FIR) missions, which makes these fluctuations potentially detectable in the near future. Emission from C II fine-structure transitions could considerably contribute to the submillimetre (submm) range of the FIR background radiation. Depending on the ionization of carbon and on the density of metal-enriched regions, this contribution can be comparable with the observed residual flux at $\lambda \approx 0.15$ mm, after CMB subtraction. We argue that constraints on metal evolution versus redshift can be obtained from the observed flux in that range.

Key words: intergalactic medium – quasars: absorption lines – cosmology: theory.

1 INTRODUCTION

Background emission from high redshift dust has been shown to be a good tracer of energy release in the early universe, since the optical properties of dust differ considerably from those of a blackbody (Rowan-Robinson, Negroponte & Silk 1979; Zinchenko 1979; Negroponte, Rowan-Robinson & Silk 1981; Bond, Carr & Hogan 1986; Naselskii & Novikov 1989; Bond, Carr & Hogan 1991; Loeb & Haiman 1997). Direct indications of the existence of dust at high redshift come from the reddening of background quasars (Ostriker & Heisler 1984; Fall & Pei 1989). Indirect evidence of dust in damped Lyα systems has been obtained from the relative gas-phase abundances of Zn and Cr (Pettini et al. 1997). Fall, Charlot & Pei (1996) have calculated the cosmic infrared background from dust in damped Lyα systems, and found good agreement with the far-infrared (FIR) background ($\nu I_\nu \approx 10^{-5}$ erg cm^{-2} s^{-1} sr^{-1} at 200–400 μm) deduced from *COBE*/FIRAS data (Puget et al. 1996; Guiderdoni et al. 1997; Fixen et al. 1998), which also seem to imply the presence of dust. The recent detection of heavy elements, such as carbon and silicon (Tytler et al. 1995; Songaila & Cowie 1996) in Lyα clouds at redshift $z \sim 3$, can potentially indicate that dust exists also in the Lyα forest: it is quite natural to assume that dust grains are associated with heavy elements. Dust in Lyα forest clouds would be relevant to the understanding of the origin of Lyα clouds and their association to Population III objects (Ciardi & Ferrara 1997), the enrichment of the intergalactic medium with metals (Gnedin & Ostriker 1997), and the thermal history of Lyα clouds (Nath, Sethi & Shchekinov 1997). Here we assume that Lyα clouds contain dust, and calculate its contribution to the submillimeter background. Our model can then be used to set limits on the epoch of dust formation (possibly related to the IGM metal-enrichment era) by comparing the calculated dust background flux with *COBE*/FIRAS data. The results are independent of the star formation history in the Universe and weakly dependent on the specific form of the heating radiation. We first (Section 2) calculate the dust temperature and opacity (Section 3); in Section 4 we calculate the expected CMB distortions by dust emission, and Section 5 contains the estimated emission from polycyclic aromatic hydrocarbons (PAH) and metals in the gas phase. Section 6 is devoted to the study of CMB anisotropies induced by dust in Lyα clouds clustered on large scales; finally, Section 7 summarizes the results.

⋆ E-mail: ferrara@arcetri.astro.it (AF); biman@rri.ernet.in (BN); sethi@iap.fr (SKS); yus@rsuss1.rnd.runnet.ru (YS)

© 1999 RAS

2 Lyα CLOUD DUST TEMPERATURE

A dust grain in a Lyα cloud is exposed to the UV–optical background radiation (UVB) provided by high-redshift QSOs (and possibly star-forming galaxies, Loeb & Haiman 1997, neglected here), and to the cosmic microwave background (CMB). Hence, the grain will be heated to an equilibrium temperature, T, and will itself radiate. The intensity of radiation, $I_\nu(t)$, observed at epoch t is the sum of the contribution from the CMB and UVB, both attenuated by dust, and from dust emission. This is obtained by solving the radiative transfer equation in an expanding universe (Rowan-Robinson et al. 1979; Negroponte et al. 1981),

$$I_\nu(t) = \left\{\pi B_\nu[T_{\rm CMB}(t)] + \pi J_\nu(t)\right\}{\rm e}^{-\tau_\nu(t_i,t)} + \int_{t_i}^{t} \pi B_\nu[T(s)R(s)/R(t)]{\rm e}^{-\tau_\nu(s,t)}{\rm d}\tau_\nu(s,t) \tag{1}$$

where πB_ν is the Planck function in units of erg cm^{-2} s^{-1} Hz^{-1}, $T_{\rm CMB}$ is the cosmic microwave background temperature, and $4\pi J_\nu$ is the intensity of the UVB in the same units as πB_ν; R is the scalefactor, t_i (z_i) is the maximum (minimum) between the time (redshift) of dust formation and IGM reionization due to the UVB; $\tau_\nu(t_1, t_2)$ is the optical depth at epoch t_1 to a source emitting at epoch t_2.

The dust temperature at redshift z is given by the detailed balance equation

$$\int_0^\infty {\rm d}\nu Q_{\rm abs}(\nu, a)\pi B_\nu[T(z)] = \int_0^\infty {\rm d}\nu Q_{\rm abs}(\nu, a) I_\nu(z), \tag{2}$$

or

$$\int_0^\infty {\rm d}\nu Q_{\rm abs}(\nu, a)\pi\left\{B_\nu[T(z)] - B_\nu[T_{\rm CMB}(z)]\right\}{\rm e}^{-\tau_\nu(z,z_i)} \simeq \int_0^\infty {\rm d}\nu Q_{\rm abs}(\nu, a)\pi J_\nu(z){\rm e}^{-\tau_\nu(z,z_i)} \equiv \mathcal{H}(z, a). \tag{3}$$

$Q_{\rm abs}(\nu, a)$ is the absorption coefficient for a grain of radius a. We have neglected in equation (3) the effect of re-radiation from grains: this is a good approximation as long as $\tau \ll 1$. We will show in the next section that this is indeed the case for the present problem. For the same reason the attenuation both of the CMB and UVB fluxes can be neglected. In this limit the formal solution of equation (3) is

$$T(z) = \left[T_{\rm CMB}^6(z) + \Theta\frac{\mathcal{H}(z, a)}{a}\right]^{1/6}, \tag{4}$$

where $\Theta = c^4h^5/2\pi Q_{\rm abs}^0 k_B^6\Gamma(6)\zeta(6)$. In deriving equation (4) we have used the following approximation for the absorption coefficient at infrared wavelengths: $Q_{\rm abs}(\nu, a) = Q_{\rm abs}^0 a\lambda^{-2}$ with $Q_{\rm abs}^0 = 1.182\times10^{-2}$ cm; this is an excellent fit to the results of Draine & Lee (1984) for the astronomical silicate for $\lambda \gtrsim 20$ μm; ζ is the Riemann function, and other symbols appearing in Θ have the usual meaning. Thus, the evolution of the dust temperature excess over $T_{\rm CMB}$ is governed by the UVB energy flux absorbed by the grain, $\mathcal{H}(z, a)$. In order to determine this quantity we have adopted the Haardt & Madau (1996, hereafter HM) UVB spectrum, and convolved it with the $Q_{\rm abs}(\nu, a)$ as calculated from optical properties of Draine & Lee (1984) astronomical silicates for a given value of a, in the wavelength range 4.3 Å $\leq \lambda \leq$ 48 μm. This choice tends to underestimate the true UVB flux for two reasons: (i) possible contributions from galaxies in addition to quasars have not been included; (ii) the power-law approximation to the typical UV–optical spectrum of a quasar does not account for line emission and other features, such as the well known blue bump. Thus, equation (4) represents a lower limit to $T(z)$. In addition, if a population of very small grains and/or PAHs does exist in Lyα clouds, the grain temperature might fluctuate stochastically. The equilibrium approximation breaks down when the temperature fluctuation ΔT is $(\langle\Delta T^2\rangle)^{1/2}/T \sim 1$: according to Draine & Anderson (1985) this should occur for $a \lesssim 20$ nm, both for silicate and graphite grains. In general this non-equilibrium effect mimics a higher equilibrium temperature.

We have solved equation (4) numerically, and the following analytical expression approximates the numerical results within less than 5 per cent on the entire redshift range for which the UVB data exist, $0 \leq z \leq 6$:

$$\frac{T(z) - T_{\rm CMB}(z)}{T_{\rm CMB}(z)} = \frac{\Delta T}{T_{\rm CMB}} \approx 0.54{\rm e}^{-1.36z}a_{\rm nm}^{-0.37}, \tag{5}$$

where $a_{\rm nm} = a$/nm. The previous formula demonstrates that the dust temperature is governed by the CMB at high redshift ($\Delta T/T_{\rm CMB}[z > 3] \lesssim 0.1$ per cent for a 100 nm grain, and therefore the presence of the UVB is completely negligible at these earlier epochs), and that larger grains tend to be slightly colder, since they are more efficient emitters.

3 DUST OPACITY

The dust optical depth at redshift z_1 to a source emitting at redshift z_2 is (Rowan-Robinson et al. 1979)

$$\tau_\nu(z_1, z_2) = c\int_{z_1}^{z_2} \rho_{\rm c}\Omega_{\rm d}^{{\rm Ly}\alpha}(z)\kappa(\nu, a)\left|\frac{{\rm d}t}{{\rm d}z}\right|{\rm d}z, \tag{6}$$

where $|{\rm d}t/{\rm d}z| = H_0^{-1}(1+z)^{-5/2}$ (we assume a cosmology with $\Omega = 1$, and $h = 0.65$, wherever this is not otherwise specified); $\Omega_{\rm d}^{{\rm Ly}\alpha}$ is the mass density of dust in Lyα clouds in units of the cosmological critical density, $\rho_{\rm c}$, and $\kappa = 3Q_{\rm abs}/4a\delta$, with $\delta \sim 3$ g cm^{-3} being the grain mass density, is the grain absorption cross-section per gram. Introducing the dust-to-gas ratio, $\mathcal{D}$, we can express the dust density in terms of the Lyα cloud baryon density as $\Omega_{\rm d}^{{\rm Ly}\alpha} = \mathcal{D}\Omega_{\rm b}^{{\rm Ly}\alpha}$. Next we assume that $\mathcal{D}$ has a power-law dependence on the gas metallicity (in solar units): $\mathcal{D} = \mathcal{D}_\odot Z^p$, where $\mathcal{D}_\odot$ gives the appropriate normalization to the galactic value. The precise determination of $\mathcal{D}_\odot$ still suffers from uncertainties related to the amount of cold ($T \leq 30$ K) dust; reasonable estimates of the latter quantity yield a value $\mathcal{D}_\odot \approx 6.7\times10^{-3}$, which we use here (Young & Scoville 1991). The index p is usually taken to be equal to unity (Pei & Fall 1995; Fall et al. 1996; Eales & Edmunds

1996), implying a linear relation between $\mathcal{D}$ and Z. However, an increasing number of studies (Issa, MacLaren & Wolfendale 1990; Schmidt & Boller 1993; Lisenfeld & Ferrara 1998) find that such a relation is non-linear. For example, Lisenfeld & Ferrara (1998) find $p = 1.85^{+1.1}_{-0.5}$ for a sample of dwarf galaxies which might be more representative of metal-poor Lyα clouds. Finally, we need to specify the metallicity evolution of Lyα clouds, $Z(z)$. A handful of metal absorption-line detections in the Lyα forest with $N_{\rm H\,I} \gtrsim 10^{14}$ cm^{-2} have now been claimed (Cowie et al. 1995; Tytler et al. 1995; Songaila & Cowie 1996); nevertheless, our understanding of this issue remains very poor. We assume that the metallicity in these objects varies as

$$Z(z) = Z_0 \left(\frac{1+z_{\rm m}}{1+z} \right)^q, \qquad q \geq 0, \tag{7}$$

and use observations to fix $Z_0 = Z(z_{\rm m}) \simeq 10^{-2}$ at the reference redshift $z_{\rm m} = 3$. Note that $q = 0$ corresponds to no evolution, whereas $q = 3.3$ gives a present solar metallicity. Using the above prescriptions, we can write

$$\Omega_{\rm d}^{{\rm Ly}\alpha}(z) = \mathcal{D}_{\odot} Z_0^p \left(\frac{1+z_{\rm m}}{1+z} \right)^{pq} \Omega_{\rm b}^{{\rm Ly}\alpha}; \tag{8}$$

we assume $\Omega_{\rm b}^{{\rm Ly}\alpha} \simeq \Omega_{\rm b}$ in agreement with recent hydrodynamical simulations (Miralda-Escudé et al. 1996). Substituting the above relation into equation (6), we derive the behaviour of $\tau_{\lambda_0}(0, z)$ (shown in Fig. 1) as a function of the present wavelength, λ_0 for different values of z and q. From Fig. 1 we deduce that: (i) the opacity in the submillimeter range is smaller than a few per cent at all redshifts $z < 20$; (ii) the opacity to UVB photons is always ≤ 0.1 if $z < 6$, the epoch for which an HM-type UVB is assumed to exist. However, the Lyα cloud dust opacity to redshift $\sim$5 sources around $\lambda_0 \sim 1$ μm is as high as $\sim$0.13, and could considerably affect observations of the distant Universe in that band.

4 CMB DISTORTION BY DUST

In this section we calculate the expected distortions of the CMB spectrum caused by dust emission with the temperature evolution as in equation (5). The observed intensity at the present epoch in the microwave range (equation 1) is

$$I_{\nu_0}(z=0) = \left\{ \pi B_{\nu_0}[T_{\rm CMB}(z)/(1+z)] \right\} [1 - \tau_{\nu_0}(0, z_i)] + \int_0^{z_i} \pi B_{\nu_0}[T(z)/(1+z)] {\rm d}\tau_{\nu_0}, \tag{9}$$

where $\nu = \nu_0(1+z)$ (ν_0 is the photon frequency at $z = 0$). We have used the strong inequality $\tau_{\nu_0}^{IR} \ll 1$, and in the third term the second-order factors in the product $\Omega_{\rm d}^{{\rm Ly}\alpha}$ have been neglected. We now compare the total intensity in equation (9) with that of CMB one. To parametrize the deviation of the CMB spectrum at $z = 0$ from a blackbody, we introduce the y parameter, defined as

$$y(z_i) \equiv \frac{1}{4} \left\{ \frac{\int_0^{\infty} {\rm d}\nu_0 I_{\nu_0}(z_i)}{\int_0^{\infty} {\rm d}\nu_0 \pi B_{\nu_0}\left[T_{\rm CMB}(z_i)/(1+z_i) \right]} - 1 \right\}; \tag{10}$$

The experimental results from *COBE* have set the upper limit, $y_C = 1.5 \times 10^{-5}$ at the 95 per cent confidence level (Fixsen et al. 1996). Using

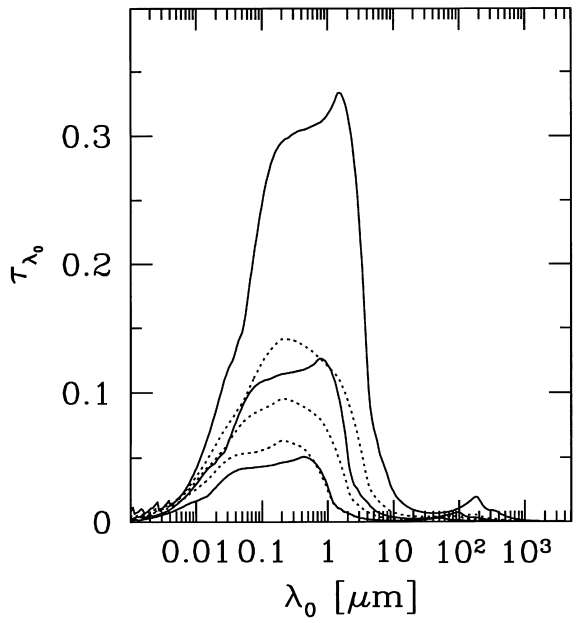

Figure 1. Dust opacity as a function of the present observation wavelength for $p = 1$, $a = 100$ nm. The curves refer to different values of the evolution parameter $q = 0$ (solid lines), 1 (dashed) and redshift $z = 5, 10, 20$ from the lowermost to the uppermost curves, respectively.

equations (5), (6) and (9), we obtain

$$y(z_i) \simeq \mathcal{A} \int_0^{z_i} \mathrm{d}z H_0 \left|\frac{\mathrm{d}t}{\mathrm{d}z}\right| (1+z)^{6-pq} \mathrm{e}^{-1.36z}, \tag{11}$$

where $\mathcal{A} = \mathcal{D}_\odot Z_0^p \left(1+z_\mathrm{m}\right)^{pq} \Omega_\mathrm{b}^{\mathrm{Ly}\alpha} a_\mathrm{nm}^{-0.37} h$. Note that y depends strongly on z_i as long as $\Delta T/T_\mathrm{CMB}$ is relatively large, but only linearly on $\Omega_\mathrm{b}^{\mathrm{Ly}\alpha}$, thus making the result robust against evolution of cloud baryon content.

Fig. 2 shows graphically the result given in equation (11) for $\Omega_\mathrm{b}^{\mathrm{Ly}\alpha} = 0.02$ and $a_\mathrm{nm} = 100$ for different values of p and q as a function of z_i. For $p = 1$, $y(z_i)$ falls below y_C by a factor 1.25–10 ($z_i \gtrsim 3$). Higher values of q (i.e. stronger metallicity evolution) produce larger values of y since more dust is present at redshifts where $\Delta T/T_\mathrm{CMB}$ is larger. For similar reasons, the case with $p = 2$ generally yields lower values of y. As a comparison we have also plotted results for two different cosmologies, i.e. a flat model with $\Omega_\Lambda = 0.4, h = 0.65$ and an open model with $\Omega = 0.2, h = 0.65$, for $p = 1, q = 0$. These two models give essentially the same curve for the y parameter, which in turn is lower than the standard case $\Omega = 1$.

5 FIR EMISSION FROM PAHs AND METALS

Small grains ($a \sim 10$–100 Å) and PAH molecules ($a \sim 5$–30 Å) are numerous in the local interstellar medium (ISM). They are traced by a strong excess of emission around 10 μm (Puget, Léger & Boulanger 1985) which arises as a result either of the temperature fluctuations of small grains, or of the characteristic IR emission of PAH molecules. We assume that physical conditions in Lyα clouds allow small grains to exist there. Although the origin of small grains is still far from being clearly understood, we note that the most efficient destruction mechanism (ionizing UV radiation) is much weaker (by at least 2.5 orders of magnitude) in Lyα clouds than in the local ISM. Following this idea, we estimate possible observational evidence for small grains and PAH molecules in Lyα clouds.

The total energy emitted by a 100-atom PAH in a band $\Delta\lambda = 0.04$ μm around the rest frame wavelength $\lambda_\mathrm{r} = 3.3$ μm can be estimated as $E_{\lambda_\mathrm{r}} \simeq 4.2$ eV (Puget & Léger 1989) per absorbed UV photon ($E_\mathrm{UV} \sim 10$ eV). The volume emissivity in this band is then

$$\mathcal{E}_\nu = \frac{E_{\lambda_\mathrm{r}}}{\Delta\lambda} \dot{N}_\mathrm{p}^\mathrm{PAH}. \tag{12}$$

$\dot{N}_\mathrm{p}^\mathrm{PAH}$ is the rate of UV photons absorbed by PAHs per unit volume

$$\dot{N}_\mathrm{p}^\mathrm{PAH} = \Phi_\mathrm{UV} \sigma_\mathrm{UV}^\mathrm{PAH} \Delta n_\mathrm{g}, \tag{13}$$

where Φ_UV is the incident UV photon flux, and $\sigma_\mathrm{UV}^\mathrm{PAH}$ is the absorption cross-section. Léger, d'Hendecourt & Défourneau (1989) give $\sigma_\mathrm{UV}^\mathrm{PAH} \simeq 2 \times 10^{-17} N_\mathrm{C}$ cm^2, with $N_\mathrm{C} \approx 30$ the number of carbons in a PAH of $a \sim 10$ Å. To estimate the number density of PAHs, Δn_g, we assume that the MRN (Mathis, Rumpl & Nordsiek 1977) grain-size distribution extends well into the domain of molecular sizes, following Tielens (1990):

$$\frac{\mathrm{d}n_\mathrm{g}}{\mathrm{d}a} = C \left(\frac{a_\mathrm{m}}{a}\right)^{3.5}, \tag{14}$$

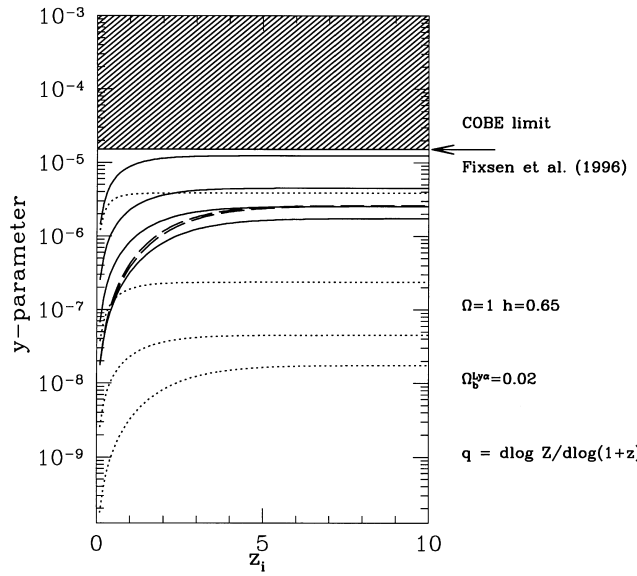

Figure 2. The equivalent y parameter versus $z_i = \min$ [reionization, dust formation redshift] produced by dust ($a = 100$ nm) in different evolutionary scenarios: $p = 1$ (solid lines), and $p = 2$ (dotted lines) for $q = 0, 1, 2, 3.3$; $\Omega_\mathrm{b}^{\mathrm{Ly}\alpha} = 0.02$. The dashed, overlapped lines refer to the cosmologies $\Omega_\Lambda = 0.4, h = 0.65$ and $\Omega = 0.2, h = 0.65$, for $p = 1, q = 0$.

where $a_{\rm m}$ is the distribution upper radius cut-off; C is a constant to be determined from

$$\int_{\rm sizes} \frac{4}{3}\pi\delta a^3 \frac{{\rm d}n_{\rm g}}{{\rm d}a}\,{\rm d}a = \mathcal{D}\Omega_{\rm b}^{{\rm Ly}\alpha}\rho_{\rm c}. \tag{15}$$

This gives

$$\Delta n_{\rm g}(a) = \frac{3}{2}\frac{\Omega_{\rm b}^{{\rm Ly}\alpha}\rho_{\rm c}}{\pi\delta a_{\rm m}^3}\left(\frac{a_{\rm m}}{a}\right)^{3.5}\Delta a. \tag{16}$$

We identify PAH molecules with grains of $a \sim 10$ Å which contain about 100 atoms (about 70 hydrogen and 30 carbon, see Puget & Léger 1989), and estimate their number density as

$$\Delta n_{\rm g} = 5.5\times10^{-9}\mathcal{D}_0 Z_0^p\left(\frac{1+z_{\rm m}}{1+z}\right)^q(1+z)^3\Omega_{\rm b}^{{\rm Ly}\alpha}\Delta a, \tag{17}$$

with $\Delta a \simeq a \approx 10^{-7}$ cm; here we have taken $a_{\rm m} = 0.1$ μm. Assuming the photon flux at $E_{\rm UV} \sim 10$ eV to be $\Phi_{\rm UV} \sim 3\times10^7$ photon s^{-1} cm^{-2} – a factor of 3 higher than the HM value at $z \approx 2-3$ to account for possible contributions from normal galaxies – we then obtain

$$\nu_0 I_{\nu_0} = \frac{c}{4\pi}\int_0^\infty {\rm d}z\left|\frac{{\rm d}t}{{\rm d}z}\right|\mathcal{E}_{(1+z)\nu_0} \simeq 2\times10^{-12}{\rm ergs^{-1}cm^{-2}sr^{-1}}. \tag{18}$$

Similar values are found for other PAH bands, i.e. $\lambda_{\rm r} = 6.2, 7.7, 8.6, 11.3$ μm. Thus the characteristic emission from PAHs in Lyα clouds is much weaker than the FIR background deduced by FIRAS, and shown in Fig. 3.

The contribution of temperature fluctuations of small grains ($a < 100$ Å) to the CMB distortion can also be shown to be unimportant. This can be seen from a comparison of the characteristic time between two subsequent absorptions of UV photons,

$$t_{\rm abs} \approx 4\times10^5\left(\frac{100{\rm Å}}{a}\right)^3{\rm s}, \tag{19}$$

and the characteristic cooling time of a grain,

$$t_{\rm cool} \approx \frac{10^4}{T_0}{\rm s}, \tag{20}$$

where the maximum temperature of a grain T_0 after absorption of a photon with energy $h\nu \approx 20$ eV is $T_0 \approx 50(100{\rm Å}/a)^{3/4}$ (Aanestad 1989). This gives

$$\frac{t_{\rm cool}}{t_{\rm abs}} \simeq 5\times10^{-4}\left(\frac{100{\rm Å}}{a}\right)^{-15/4} \ll 1. \tag{21}$$

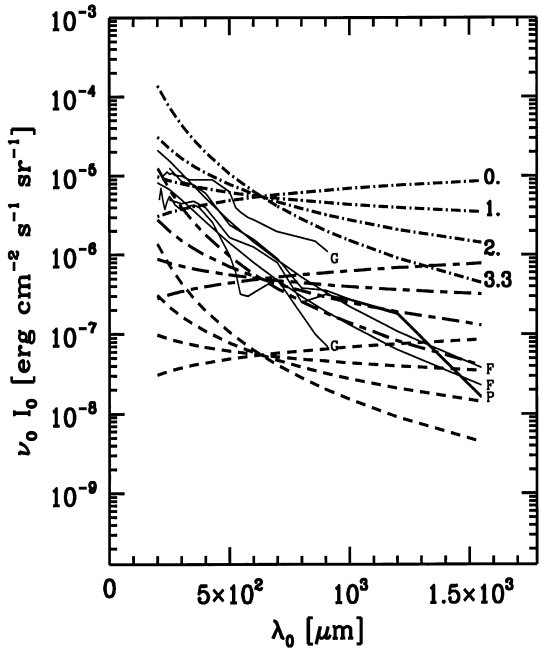

Figure 3. The FIR background and submm emission from C II ions in Lyα clouds. Solid lines show different estimates of the *COBE*/FIRAS data by Puget et al. (1996) (labelled P), Guiderdoni et al. (1997) (G), and Fixen et al. (1998) (F). Broken lines represent C II emission for different metallicity evolution: $q = 3.3, 2.0, 1.0, 0.0$, and Lyα cloud overdensity $f^{1/2}\Delta = 10^4$ (dot-dashed), $f^{1/2}\Delta = 3\times10^3$ (long dot-dashed), $f^{1/2}\Delta = 10^3$ (dashed); fractional ionization $x_{\rm C\,II} = 1$, $z_{\rm m} = 3$, $z_i = 10$.

The FIR background emission from ions in gas phase, particularly from C II (at rest-frame wavelength $\lambda_r = 158\mu$m) and Fe II (rest-frame wavelengths $\lambda_r = 26, 35$ μm) can potentially trace heavy elements in Lyα clouds. The C II emissivity per unit volume arising from collisions is (see Wolfire et al. 1995)

$$\mathcal{E}_\nu = 5\times 10^{-25} Z_0 [C] x_{\rm C\,II} T_4^{-0.18} n_e^2 (\Delta\nu_{\rm D})^{-1}, \tag{22}$$

where $\Delta\nu_{\rm D}$ is the Doppler width, $[C]$ the abundance of carbon, $x_{\rm C\,II}$ the C II ionization fraction. With the above assumptions and for solar carbon abundance, $[C] = [C]_\odot$, we obtain

$$\nu_0 I_{\nu_0} = \frac{c}{4\pi}\nu_0 \int_0^{z_i} {\rm d}z \left|\frac{{\rm d}t}{{\rm d}z}\right| \mathcal{E}_{(1+z)\nu_0} \simeq 10^{-13} h^3 f \Delta^2 \left(\frac{\Omega_{\rm b}^{\rm Ly\alpha}}{0.02}\right)^2 x_{\rm C\,II} (1+z_{\rm m})^q \left(\frac{\nu_0}{\nu_{\rm r}}\right)^{q-1/2} \Theta[\nu_0(1+z_i) - \nu_{\rm r}], \tag{23}$$

where Δ is the overdensity of Lyα clouds, and f is the filling factor of denser regions. Fig. 3 shows the expected emission from C II ions compared with the FIR background. We are plotting for completness three different estimates of the background taken from Puget et al. (1996), Guiderdoni et al. (1997), and Fixsen et al. (1998). Such emission in this case is more model dependent than the CMB distortion produced by dust particles. Aside from uncertainties connected with abundance and ionization of C II, the density of Lyα cloud gas enters as an additional free parameter because of the collisional nature of emission from C II fine-structure lines. On average, the density contrast of Lyα clouds is thought not to exceed 10–30. However, the regions containing metals and dust could be connected with debris of supershells produced by strong explosions during active star formation phases in young galaxies, and can be much more dense. In such regions the gas density can be as high as $n \sim 0.1\,{\rm cm}^{-3}$. To illustrate the dependence of the FIR background on gas density in metal-rich regions of Lyα clouds, we present in Fig. 3 the flux calculated from equation (23) for density contrasts $\Delta = 10^3, 3\times 10^3$, and 10^4 which correspond at $z = 3$ to a number density $n \simeq 0.005, 0.015$, and $0.05\ {\rm cm}^{-3}$, respectively. The intensity of C II emission is plotted for $x_{\rm C\,II} = 1$, and scales as $\propto x_{\rm C\,II}$.

Fig. 3 allows us to draw qualitative conclusions about the evolution of metals in Lyα clouds. It is seen clearly that only strong evolutionary scenarios ($q > 1$) can avoid producing an excess in the submm range of the backround radiation. In particular, $x_{\rm C\,II} = 0.01$ models with high overdensity, $f^{1/2}\Delta = 10^4$, produce an intensity below the *COBE*/FIRAS data at submm wavelengths only when $q \geq 2$. In general, this requirement is satisfied by all models with $f^{1/2}\Delta x_{\rm C\,II}^{1/2} \leq 10^3$. For realistic values $f < \Delta^{-1}$, the C II emission can exceed the *COBE*/FIRAS flux in the submm range only for overdensities $\Delta \gtrsim 10^6$.

It is also clear that Fe II ions make only a small contribution to the FIR background for two reasons: iron is less abundant than carbon, and in addition fine-structure emission of Fe II falls to the shorter wavelength range, 26 (35) $\mu{\rm m} \leq \lambda_0 \leq 26$ (35) $(1+z_i)$ μm $= 286$ (385) μm for $z_i = 10$, where the background emission is much stronger than in the submm range.

6 CMB ANISOTROPIES ARISING FROM DUST EMISSION

As the dust distribution is inhomogeneous, it will result in the anisotropy of the FIR background radiation caused by dust emission. The angular pattern of anisotropy will depend on the sizes and clustering properties of the Lyα clouds. If the Lyα clouds are assumed to be unclustered and Poisson distributed, then the typical value of anisotropy in the intensity $\simeq N^{-1/2}$, N being the average number of clouds along any given line of sight; observations show that $N \simeq 100$ up to $z \simeq 3$ (see e.g., Mo, Miralda-Escudé & Rees 1993) The angular pattern will be a 'white noise' spectrum, i.e. independent of the angle. Of course, in a realistic experiment there would be a further smearing of this anisotropy by the finite width of the beam by a factor of $x_{\rm cl}/\sigma_0$, $x_{\rm cl}$ and σ_0 being the typical size of cloud and the beam width, respectively. However, although the clustering properties of Lyα clouds remain controversial, Cristiani et al. (1997) have claimed a weak but non-negligible clustering of Lyα clouds at high redshifts. According to Cristiani et al. (1997), Lyα clouds below H I column densities $10^{13.8}\ {\rm cm}^{-2}$ show no clustering, but clouds of higher column density cluster at scales corresponding to a few hundred km s^{-1}, with a clustering amplitude proportional to the H I column density. In addition, they notice a trend of increase in clustering as the redshift decreases. Their results, cast in the form of a three-dimensional two-point correlation function, are consistent with $\xi(r) = [r/r_0(z)]^{-\gamma}$ with $\gamma = 1.77$ and $r_0(z) = r_0(0)\times(1+z)^{-5/3}$ from $1.7 \lesssim z \lesssim 4$ with $r_0(0) \simeq 1.5$–$2\ h^{-1}$ Mpc. At lower redshifts the clustering is observed to be higher than predicted by the clustering behaviour at high z (Ulmer 1996). For the purposes of this paper, we take the redshift dependence of clustering amplitude indicated by the high redshift data up to $z = 0$, bearing in mind that this might underestimate the clustering at low z.

We follow the treatment of Bond et al. (1986) in evaluating the two-point angular correlation function, $C(\theta)$, of the anisotropies from the clustering of Lyα clouds (for more details see Peebles 1993). For the three-dimensional two-point correlation function given above, we obtain

$$C^{1/2}(\theta) = \frac{\langle \Delta I_{\rm d}^2(\theta)\rangle^{\frac{1}{2}}}{\langle I_{\rm d}\rangle} \simeq F_{pq}(z_i) \left[\frac{H_0 r_0(0)}{2c}\right]^{\frac{\gamma}{2}} \sin^{\frac{1-\gamma}{2}}\theta, \tag{24}$$

where $\langle I_{\rm d}\rangle$ is the mean intensity of the background emission from dust. $F_{pq}(z_i) \simeq 1$, and it increases slightly as z_i is decreased and/or the product pq is increased, indicating that the dominant signal comes from a smaller redshift where the clustering scale is larger. For $\gamma \simeq 1.77$ and $H_0 r_0(0) \simeq 150\,{\rm km\ s}^{-1}$, we get $\langle \Delta I_{\rm d}^2\rangle^{1/2}/\langle I_{\rm d}\rangle \simeq 1.1\times 10^{-3}\theta^{-0.4}$ for $\theta \ll 1$. At $\theta \simeq 10$ arcsec, the angle corresponding to the typical clustering scale at high z, $\langle \Delta I_{\rm d}^2\rangle^{1/2}/\langle I_{\rm d}\rangle \simeq 0.1$, which is comparable to what one would expect from the 'white noise' fluctuations discussed above. We recall that equation (24) should not be used for scales smaller than the typical size of the cloud at high z. The signal from dust emission will be significant at wavelengths $\simeq$400–1000 μm, with typical intensities $\simeq 10^{-7}$–$10^{-8}\ {\rm erg\,cm^{-2}\,s^{-1}\,sr^{-1}}$, with a fluctuation amplitude of 0.1 at angular scales 10 arcsec–1 arcmin. The ongoing and future missions like *ISO* (*ISO*-PHOT), SCUBA, and *FIRST* operate/will operate in this

wavelength band with sensitivities high enough to detect this fluctuation, though it may be hard to separate the contribution of Lyα cloud dust emission from other extragalactic sources at high redshift.

Another potentially measurable quantity is the predicted CMB anisotropy. The latter is given by the ratio of the angular intensity variation to the CMB radiation at any given frequency:

$$\frac{\langle \Delta I_{\rm d}^2(\theta)\rangle^{1/2}}{\langle I_{\rm CMB}\rangle} = \frac{3.55\times10^{-8}}{11-2pq} Z_0^p \left(\frac{\Omega_{\rm b}^{\rm Ly\alpha}}{0.02}\right)(1+z_{\rm m})^{pq}\left(\frac{\nu_0}{10^{11}\,{\rm Hz}}\right)^2 \left[(1+z_i)^{-pq+11/2}-1\right]\frac{\langle \Delta I_{\rm d}^2(\theta)\rangle^{1/2}}{\langle I_{\rm d}\rangle}. \quad (25)$$

Taking $z_i = 5$, $p = q = 0$, and $\Omega_{\rm b}^{\rm Ly\alpha} = 0.02$, we get $\langle \Delta I_{\rm d}^2(\theta)\rangle^{1/2}/\langle I_{\rm CMB}\rangle \simeq 9.2\times10^{-6}h^{-1}\langle \Delta I_{\rm d}^2(\theta)\rangle^{1/2}/\langle I_{\rm d}\rangle$ at $\nu_0 = 360\,{\rm GHz}$. Most of the contribution to the anisotropy comes from high redshifts (around $z = z_i$) where most of the baryons are seen to be in Lyα clouds in recent hydrodynamical simulations (Miralda-Escudé et al. 1996). Fomalont et al. (1993) obtained an upper bound of $\Delta T/T_{\rm CMB} < 3\times10^{-5}$ for 10−100 arcsec at $\nu_0 = 8.44\,{\rm GHz}$. The anisotropies from dust emission are several orders below this upper limit because of their ν_0^2 dependence. The best hope of detecting the anisotropy is at infrared frequencies. Recently, the ongoing CMB experiment – the Sunyaev–Zel'dovich infrared experiment (SuZIE) – reported its first results. At $\nu = 142\,{\rm GHz}$, they obtained an upper limit $\Delta T/T \leq 2.1\times10^{-5}$ at angular scales of ≃1.1 arcmin (Church et al. 1997). A comparison of this result with our estimate shows that our predictions are still an order below this upper limit. However, in coming years, the SuZIE instrument will be upgraded to have additional frequency channels at 217 and 268 GHz. As the expected signal is much higher at these frequencies, it might be marginally detectable. Also, this anisotropy might be an important foreground for other secondary CMB anisotropies which could be present at sub-arcminute scales with amplitudes of a few μ K (for details see Bond 1996 and references therein). The future CMB mission, the Planck surveyor, will also operate at frequencies at which the dust emission from high-z Lyα clouds will peak (see Bouchet, Gispert & Puget 1995). With its sensitivity, the Planck surveyor will be able to detect a fluctuation at the level of a few μK at $\nu_0 \simeq 300\,{\rm GHz}$ with an angular resolution of 4.5 arcmin. From our analysis above, the fluctuations expected from dust emission are likely to be weaker than the sensitivity of the Planck surveyor.

7 CONCLUSIONS

We have considered possible observational consequences of the presence of dust in Lyα clouds. We have used a rather general expression for the dust density, $\rho_{\rm d}(z) = \rho_{\rm c}\mathcal{D}_0 Z_0^p (1+z_{\rm m}/1+z)^{pq}\Omega_{\rm b}^{\rm Ly\alpha}(z)$, which accounts for the possible non-linearity of the dust-to-metals ratio versus metallicity (Lisenfeld & Ferrara 1998), and the evolution of metallicity with z. We have calculated the temperature of dust grains heated by CMB photons and UV background radiation from quasars following Haardt & Madau (1996), and assuming dust to be constituted of standard 'astronomical silicates' (Draine & Lee 1984). Our main results are the following.

(1) The contribution of UV radiation to dust heating is small in comparison with heating by CMB photons; only at $z \leq 1$ does the dust temperature fractional deviation from $T_{\rm CMB}(z)$ reach its maximum of 5–10 per cent.

(2) The Lyα cloud dust opacity to redshift ∼5 sources around the observed wavelength $\lambda_0 \sim 1\mu{\rm m}$ is $\tau \sim 0.13$.

(3) The expected CMB spectral distortion arising from high-z dust in Lyα clouds is ∼1.25−10 smaller than the current *COBE* upper limit on the y parameter, depending on the metallicity evolution.

(4) The predicted value of anisotropies produced by dust clustered on scales $H_0 x_0 \sim 150\,{\rm km\,s^{-1}}$ is $\langle \Delta I_{\rm d}^2(\theta)\rangle^{1/2}/\langle I_{\rm d}\rangle \simeq 0.1$ on scales $\theta \lesssim 10$ arcsec. The ongoing and future missions operating at FIR wavelengths might be able to detect such an effect, thus providing valuable information on the dust content, evolution and clustering properties of Lyα clouds.

(5) The fine-structure emission of C II ions can contribute to the submm range of the spectrum if metal-enriched regions in Lyα clouds are sufficiently dense, $n \sim 0.1\,{\rm cm^{-3}}$. If the average overdensity in such regions is as high as $\Delta \gtrsim 10^3/(f x_{\rm CII})^{1/2}$, only strong metallicity evolutionary scenarios with $q > 1$ are allowed.

ACKNOWLEDGMENTS

We thank the referee, Dr F. Bouchet, for insightful comments. SKS thanks Bruno Guiderdoni for useful information on FIR missions. YS acknowledges support from NATO Guest Fellowship Programme 1996 from Italian CNR 219.29.

REFERENCES

Aanestad P. A., 1989, in Bonetti A., Greenberg J. M., Aiello S., eds, Evolution of Interstellar Dust and Related Topics, Societã Italiana di Fisica, Bologna, p. 121
Bond J. R., 1996, in Schaeffer R., ed., Cosmology and Large-Scale Structure in the universe. Elsevier, Les Houches, p. 469
Bond J. R., Carr B. J., Hogan C. J., 1986, ApJ, 306, 428
Bond J. R., Carr B. J., Hogan C. J., 1991, ApJ, 367, 420
Bouchet F. R., Gispert R., Puget J.-L., 1996, in Dwek E., ed., AIP Conf. Proc. 348, The mm/sub-mm foregrounds and future CMB Space Missions. AIP Press, New York, p. 255.
Church S. E., Ganga K. M., Ade P. A. R., Holzapfel W. L., Mauskopf P. D., Wilbanks T. M., Lange A. E., 1997, ApJ, 484, 523
Ciardi B., Ferrara A., 1997, ApJ, 483, L5
Cowie L. L., Songaila A., Kim. T., Hu E. M., 1995, AJ, 109, 1522
Cristiani S., D'Odorico S., D'Odorico V., Fontana A., Giallongo E., Savaglio S., 1997, MNRAS, 285, 209
Draine B. T., Anderson N., 1985, ApJ, 292, 494
Draine B. T., Lee H. M., 1984, ApJ, 258, 89

Eales S. A., Edmunds M. G., 1996, MNRAS, 280, 1167
Fall S. M., Pei Y. C., 1989, ApJ, 341, L5
Fall S. M., Charlot S., Pei Y. C., 1996, ApJ, 464, L43
Fixsen D. J., Cheng E. S., Gales J. M., Mather J. C., Shafer R. A., Wright E. L., 1996, ApJ, 473, 576
Fixsen D. J., Dwek E., Mather J. C., Bennett C. L., Shafer R. A., 1998, ApJ, in press (astro-ph/9803021)
Fomalont E. B., Partridge R. B., Lowenthal J. D., Windhorst R. A., 1993, ApJ, 404, 8
Gnedin N. Y., Ostriker J. P., 1997, ApJ, 486, 581
Guiderdoni B., Bouchet F. R., Puget J. L., Lagache G., Hivon E., 1997, Nat, 390, 257
Haardt F., Madau P., 1996, ApJ, 461, 20 (HM)
Issa M. R., MacLaren I., Wolfendale A. W., 1990, A&A, 236, 237
Léger A., d'Hendecourt L. B., Défourneau D., 1989, A&A, 216, L148
Lisenfeld U., Ferrara A., 1998, ApJ, 496, 145
Loeb A., Haiman Z., 1997, ApJ, 490, 571
Mathis J. S., Rumpl W., Nordsiek K. H., 1977, ApJ, 217, 425
Miralda-Escudé J., Cen R., Ostriker J. P., Rauch M., 1996, ApJ, 471, 582
Mo H. J., Miralda-Escudé J., Rees M. J., 1993, MNRAS, 264, 705
Naselskii P. D., Novikov I. D., 1989, SvA, 33, 350
Nath B., Sethi S., Shchekinov, Yu., 1998, MNRAS, in press (astro-ph/9810080)
Negroponte J., Rowan-Robinson M., Silk J., 1981, ApJ, 248, 38
Ostriker J. P., Heisler J., 1984, ApJ, 278, 1
Peebles P. J. E., 1993, Principles of Physical Cosmology. UniPress, Princeton NJ
Pei Y. C., Fall S. M., 1995, ApJ, 454, 69
Pettini M., King D. L., Smith L. J., Hunstead R. W., 1997, ApJ, 478, 536
Puget J. -L., Léger A., 1989, ARA&A, 27, 161
Puget J. -L., Léger A., Boulanger F., 1985, A&A, 142, L19
Puget J. -L. et al., 1996, A&A, 308, L5
Rowan-Robinson M., Negroponte J., Silk J., 1979, Nat, 281, 635
Schmidt K. H., Boller T., 1993, Astron. Nachr., 314, 361
Songaila A., Cowie L. L., 1996, AJ, 112, 335
Tielens A. G. G. M., 1990, in Watt G. D., Webster A. S., eds, Submillimetre Astronomy. Reidel, Dordrecht, p. 13
Tytler D., Fan X. M., Burles S., Cottrell L., Davis C., Kirkman D., Zuo L., 1995, in Meylan G., ed., Proc. ESO Workshop, QSOs Absorption Lines. Springer, Heidelberg
Ulmer A., 1996, ApJ, 473, 110
Wolfire M. G., Hollenbach D., McKee C. F., Tielens A. G. G. M., Bakes E. L. O., 1995, ApJ, 443, 152
Young J. S., Scoville N. Z., 1991, ARA&A, 29, 581
Zinchenko I. I., 1979, Pis'ma AZh, 5, 435

This paper has been typeset from a $\TeX$/$\LaTeX$ file prepared by the author.